

A reconstruction of the last glacial maximum (LGM) ice-surface geometry in the western Swiss Alps and contiguous Alpine regions in Italy and France

Autor(en): **Kelly, Meredith / Buoncristiani, Jean-François / Schlüchter, Christian**

Objektyp: **Article**

Zeitschrift: **Eclogae Geologicae Helvetiae**

Band (Jahr): **97 (2004)**

Heft 1

PDF erstellt am: **21.07.2024**

Persistenter Link: <https://doi.org/10.5169/seals-169097>

Nutzungsbedingungen

Die ETH-Bibliothek ist Anbieterin der digitalisierten Zeitschriften. Sie besitzt keine Urheberrechte an den Inhalten der Zeitschriften. Die Rechte liegen in der Regel bei den Herausgebern.

Die auf der Plattform e-periodica veröffentlichten Dokumente stehen für nicht-kommerzielle Zwecke in Lehre und Forschung sowie für die private Nutzung frei zur Verfügung. Einzelne Dateien oder Ausdrucke aus diesem Angebot können zusammen mit diesen Nutzungsbedingungen und den korrekten Herkunftsbezeichnungen weitergegeben werden.

Das Veröffentlichen von Bildern in Print- und Online-Publikationen ist nur mit vorheriger Genehmigung der Rechteinhaber erlaubt. Die systematische Speicherung von Teilen des elektronischen Angebots auf anderen Servern bedarf ebenfalls des schriftlichen Einverständnisses der Rechteinhaber.

Haftungsausschluss

Alle Angaben erfolgen ohne Gewähr für Vollständigkeit oder Richtigkeit. Es wird keine Haftung übernommen für Schäden durch die Verwendung von Informationen aus diesem Online-Angebot oder durch das Fehlen von Informationen. Dies gilt auch für Inhalte Dritter, die über dieses Angebot zugänglich sind.

A reconstruction of the last glacial maximum (LGM) ice-surface geometry in the western Swiss Alps and contiguous Alpine regions in Italy and France

MEREDITH A. KELLY^{1*}, JEAN-FRANÇOIS BUONCRISTIANI² & CHRISTIAN SCHLÜCHTER¹

Key words: Glacial trimline, ice-erosional features, last glacial maximum (LGM), western Swiss Alps, geographic information system (GIS), paleoglaciology

ABSTRACT

A reconstruction of the last glacial maximum (LGM) ice-surface geometry in the western Swiss Alps and contiguous Alpine regions in Italy and France is based on detailed field mapping of glacial trimlines, ice-erosional features and periglacial forms. Field data provide evidence of LGM ice-surface elevations and ice-flow directions. The LGM ice surface is portrayed as a grid-format digital elevation model (DEM) using geographic information system (GIS) software. LGM ice-surface areas and ice volumes in selected regions are calculated using a DEM of the present land topography. The reconstruction described in this paper is presented in conjunction with a previously determined LGM ice-surface reconstruction for the central and eastern Swiss Alps.

The LGM ice cap in the western Swiss Alps and contiguous Alpine regions in Italy and France was characterized by transection glaciers. Four main centers of ice accumulation that influenced the transection glaciers include the Rhône ice dome, the Aletsch icefield, the southern Valais icefield, and the Mt. Blanc region. Major ice diffluences were located north of Simplon Pass, on Gd. St. Bernard Pass and north of present-day Glacier d'Argentière. Estimates of LGM ice volumes in selected regions show that the largest input of ice into the Rhône Valley was from the southern Valais icefield. Centered in the southern Matternal, the LGM southern Valais icefield had a surface elevation of at least 3010 m and an ice thickness of at least 1400 m. The LGM ice-surface reconstruction and calculated ice volumes for selected regions are the basis for a hypothesis as to how erratic boulders from the southern Valais and Mt. Blanc regions were transported to the northern Alpine foreland. Certain LGM centers of ice accumulation and ice-flow directions presented in this paper are also examined for possible paleo-atmospheric circulation information.

ZUSAMMENFASSUNG

Die Rekonstruktion der Eisoberflächengeometrie während des Letzten Glazialen Maximums (LGM) in den westlichen Schweizer Alpen und in angrenzenden Regionen in Italien und Frankreich basiert auf einer detaillierten Kartierung von Gletscherschliffgrenzen, Eiserosionserscheinungen und periglazialen Formen. Diese Geländedaten geben Hinweise auf die Höhe der Eisoberfläche und die Eisflussrichtungen. Die Eisoberfläche wird durch ein gitterbasiertes digitales Höhenmodell (DHM) unter Benutzung eines Geographischen Information Systems (GIS) dargestellt. Die Eisoberflächenerstreckung und die Eismächtigkeiten werden auf Basis des DHM der gegenwärtigen Landestopographie berechnet. Die in dieser Veröffentlichung beschriebene Rekonstruktion wird mit früheren Eisoberflächenrekonstruktionen für das LGM der zentralen und östlichen Schweizer Alpen verglichen.

Die Eiskappe während des LGM in den westlichen Schweizer Alpen und in angrenzenden Regionen in Italien und Frankreich war durch ein Eisstromnetz charakterisiert. Die vier Zentren der Eisakkumulation, welche das Eisstromnetz beeinflussten, waren der Rhône Eisdom, das Aletsch Eisfeld, das Eisfeld im südlichen Wallis und die Mont Blanc Region. Drei Hauptdiffuenzen des Eises lagen nördlich des Simplon Passes, auf dem Gd. St. Bernard Pass and nördlich des heutigen Glacier d'Argentière. Die Abschätzung der Eismächtigkeit zeigt dass der größte Eintrag von Eis in das Rhônetal vom Eisfeld im südlichen Wallis stammte. Mit einem Mittelpunkt im südlichen Matternal lag die Oberfläche dieses Eisfeldes in einer Höhe von mindestens 3010 m und hatte eine Eismächtigkeit von mindestens 1400 m. Die Rekonstruktion der Eisoberfläche und die berechneten Eismächtigkeiten sind die Grundlage für eine Hypothese, mit welcher der Transport von erratischen Blöcken aus dem Südwallis und der Mont Blanc Region in das Alpenvorland erklärt wird. Die verschiedenen Zentren der Eisakkumulation und die Eisströmungsrichtungen werden zudem in Bezug auf die darin enthaltene Information bezüglich der atmosphärischen Zirkulation während des LGM betrachtet.

Introduction

The former extents of Swiss Alpine glaciers have been investigated for nearly 200 years, since the founding of ancient glacial studies by Jean Pierre Perraudin, Ignace Venetz (1822, 1829) and Louis Agassiz (1837). Early portrayals of a large ice cap in the Alps, which extended onto the Alpine forelands, include

those by de Charpentier (1841), Favre (1884), Penck & Brückner (1909), Frei (1912) and Beck (1926). The most widely cited detailed reconstruction of the last maximum ice cap in Switzerland is based on a compilation of local studies of moraines and erosional features published by Jäckli (1962, 1970) (Fig. 1). Re-

¹ Institute of Geological Sciences, University of Bern, Baltzerstrasse 1, CH-3011 Bern, Switzerland

² Université de Bourgogne, UMR 5561 Biogéosciences (équipe D), 6 bd Gabrie, F-21000 Dijon, France

*Present address: Byrd Polar Research Center, The Ohio State University, 1090 Carmack Road, Scott Hall 108, Columbus, OH 43210-1002, USA.

Email: kelly.438@osu.edu.

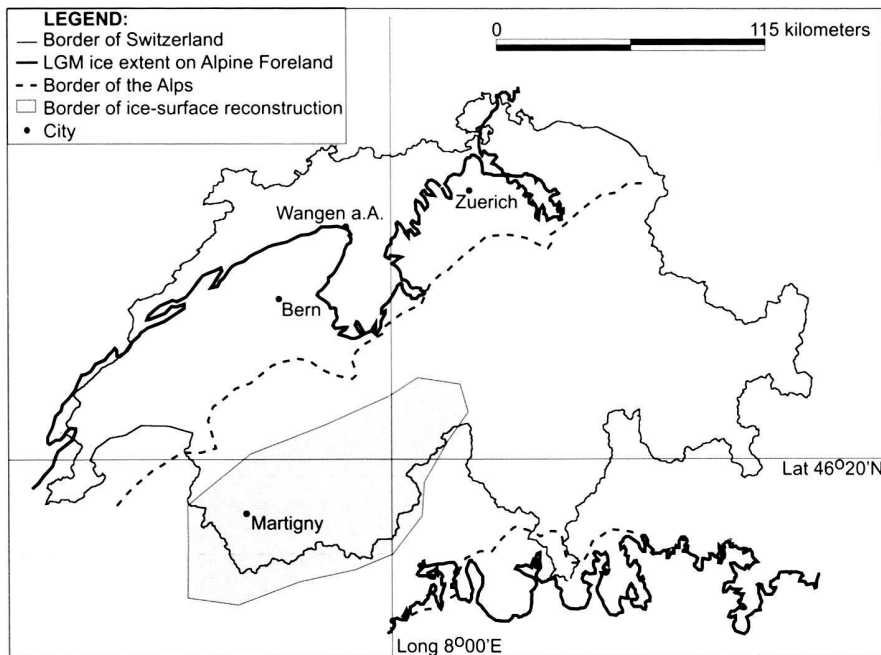


Fig. 1. Location diagram showing the extent of glaciation on the Alpine forelands during the LGM (after Jäckli 1970). Also shown is the border of the ice-surface reconstruction.

search by van Husen (1987), de Beaulieu et al. (1991) and Campy & Arn (1991) extend the ice cap reconstruction into the eastern and southwestern Alps, respectively.

Most studies portray the last maximum ice cap in the inner-Alpine region as an “ice-stream network” and, on the northern and southern Alpine forelands, as large piedmont glaciers (Jäckli 1962; Haerberli & Penz 1985). However, a recent detailed reconstruction shows that the former accumulation zone in the central and eastern Swiss Alps was not a simple network of valley glaciers, which generally followed the pre-existing land topography, but instead was characterized by ice domes (Florineth 1998). Three ice domes, or centers of ice accumulation, existed in the central and eastern Swiss Alps (Florineth & Schlüchter 1998). Ice flowed outward from the domes in a radial pattern, independent of the pre-existing valley system. The locations of the ice domes are interpreted to reflect areas of high precipitation and are related to paleo-atmospheric circulation patterns (Florineth & Schlüchter 1998, 2000).

As a continuation of the mapping in the central and eastern Swiss Alps, we present an ice-surface reconstruction of the last maximum ice cap for the inner-Alpine region of western Switzerland and for contiguous Alpine regions in Italy and France (hereinafter referred to as the western Alps). The ice-surface reconstruction is based on detailed field mapping of glacial erosional features and digital map analysis using geographic information system (GIS) software.

Study area

Within Switzerland, mapping of glacial erosional features was concentrated in Canton Valais west of Fiesch, in particular in

the regions south of the Rhône Valley (Figs. 1, 2). Research was also conducted in Valpelline, Val Veny and Val Ferret, Italy, and on the northern side of Mt. Blanc in France.

Regional geography

The upper Rhône Valley dissects the western Swiss Alps, generally trending to the southwest (Fig. 2). Its headwaters are the Rhône Glacier, near Gletsch. In Martigny, the Rhône River bends to the north-northwest and flows approximately 40 km to drain into Lake Geneva. North of the Rhône Valley, mountain peaks in the Aletsch Glacier region, such as Jungfrau, Mönch and Eiger, are as high as 4000 m. The Aletsch Glacier is about 24 km long and its meltwater outflow, the Massa River, enters the Rhône Valley at Brig. South of the Rhône Valley, the Valaisian Alps comprise the highest topography in Switzerland. Mountains such as Monte Rosa (4634 m), Matterhorn, (4478 m), and Grand Combin (4314 m) mark the geographic border between Switzerland and Italy. Long north-trending valleys, such as Saastal and Matternal, dissect the high Valaisian Alps and drain into the Rhône Valley. Two major alpine passes, Simplon and Gd. St. Bernard, are north-south openings through the Valaisian Alps from Switzerland to Italy.

Located on the border of France and Italy, Mt. Blanc (4807 m) is the highest mountain peak in the Alps (Fig. 2). The Mt. Blanc region encompasses numerous high mountains, such as Aiguille d'Argentière (3901 m) and Mt. Dolent (3820 m). Outlet glaciers including Mer de Glace and Glacier d'Argentière exit the Mt. Blanc region to the north. With its headwaters at Glacier du Tour, the Arve River drains the Mt. Blanc region to the northwest, joining the Rhône River in Geneva. The Mt.

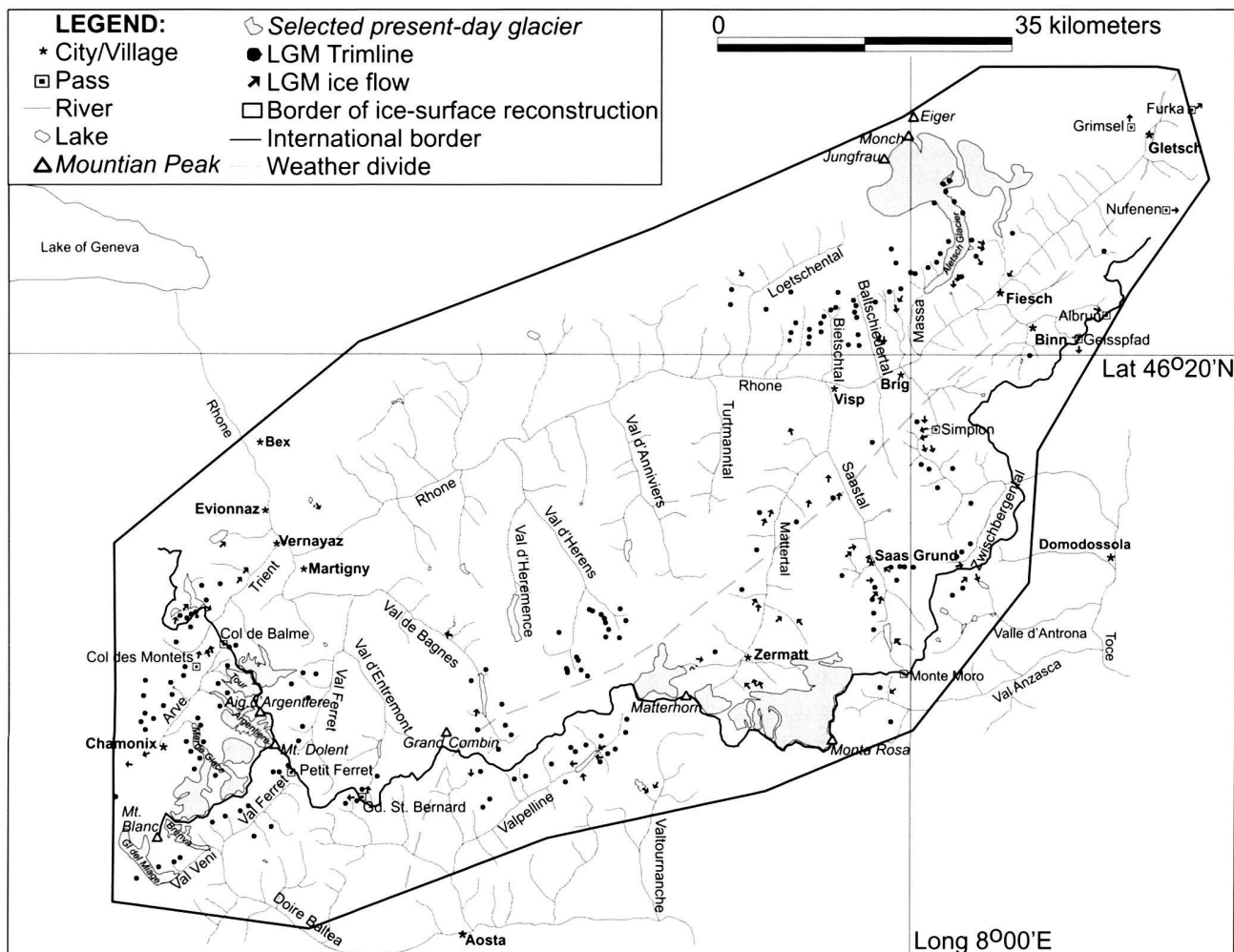


Fig. 2. Detailed location diagram of the study area. Locations discussed in the text are highlighted. Also shown is the present weather divide, according to Fliri (1984).

Blanc region is bounded to the south by the northeast trending Val Veny and Val Ferret. Glaciers del Miage and della Brenva flow south, into Val Veny. The Dora Báltea River drains Val Veny and Val Ferret, following the Val d'Aosta to the Po River.

Glaciers are prevalent in the Valais and the Mt. Blanc region because of the high-elevation topography and the influence of both (north)westerly and south/southwesterly atmospheric circulation patterns. For example, the Canton Valais encompasses 41.5 percent of the glaciers in Switzerland. Approximately 520 km² of land surface in the Valasian Alps (Maisch et al. 2000) and 170 km² of land surface in the Mt. Blanc region is glaciated. Most Alpine glaciers are temperate and are therefore erosive at the base, shaping the underlying topography. However, cold-based ice exists at high elevations (>3600 m) and where glacier tongues are thin and/or have a north or west exposition (Haerberli 1976).

Regional and Alpine climate

The regional climate of northern and central Europe is influenced by the proximity of the Atlantic Ocean and the Northern Hemisphere westerly storm tracks. The continentality of the climate in Europe generally increases eastward. The Alps are an orographic barrier and separate a southern Mediterranean climate from a northern central European climate.

At present, most precipitation in the Alps is the result of two main circulation patterns, (north)westerly and south/southwesterly. The (north)westerly circulation is dominant and is responsible for more than 22% of total annual precipitation, as opposed to the south/southwesterly circulation, which contributes about 16% (Fliri 1984). However, a weather divide marks the boundary between the areas of influence of the two circulation patterns (Fig. 2). In the western Alps, the weather divide follows approximately the Rhône Valley, with most precipitation north of the valley and in the western Valais and

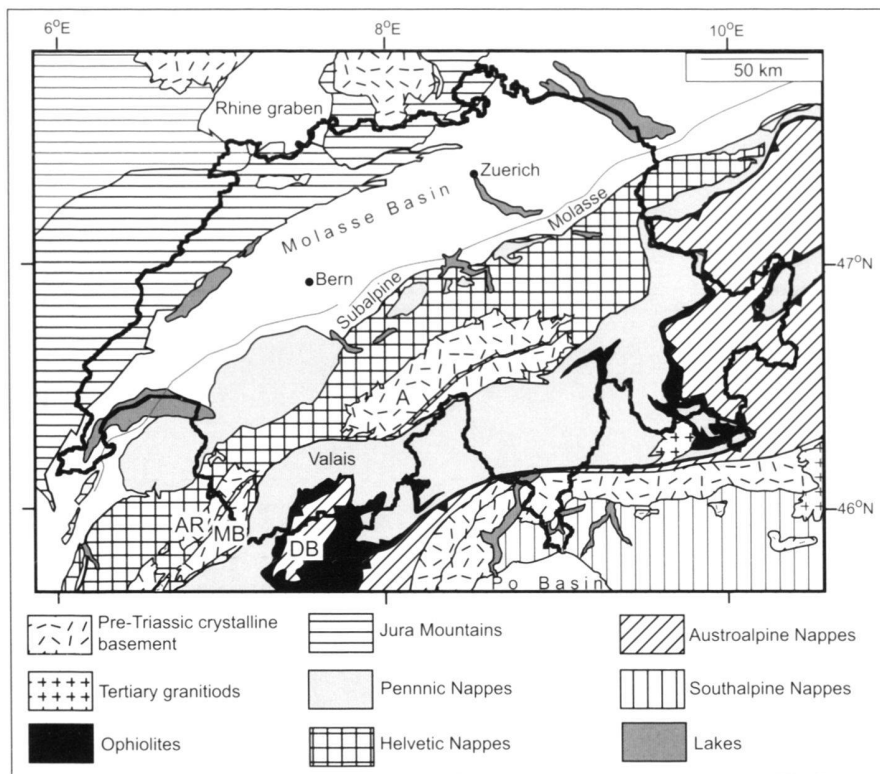


Fig. 3. General tectonic map of Switzerland (after Kühni & Pfiffner 2001). Solid line: border of Switzerland, A: Aar Massif, AR: Aiguilles Rouges Massif, MB: Mt. Blanc Massif, DB: Dent Blanche Nappe.

Mt. Blanc region due to (north)westerly circulation (Fliri 1984). The upper Rhône Valley, also known as the Goms, and the middle Valaisian Alps, including Simplon Pass and the southern ends of Saastal and Mattertal, receive most precipitation from south/southwesterly circulation (Fliri 1984).

The influence of the two main weather patterns on the east-west trending Alps results in high precipitation on the northern and southern edges of the Alps and low precipitation in the inner-Alpine valleys (Widmann & Schär 1997). The Rhône Valley at low elevation (400–700 m) is warm and dry, with a mean annual temperature of 10 °C and mean annual precipitation of 500–700 mm (Schüepp 1965). Precipitation increases at higher elevations to the north and south of the Rhône Valley. For example, on Gd. St. Bernard Pass (2479 m), mean annual temperature is –1.2 °C and mean annual precipitation is about 2000 mm (Schüepp 1965).

Bedrock geology

The study of glacial erosional forms is intimately related to an understanding of the bedrock geology. A brief overview of the major lithologic units and structural contacts within the study area is provided below. Much more detailed explanations are located in Déverin (1936), Labhart (1977), Trümpy (1980a, 1980b), Escher et al. (1993, 1997) and references therein.

The southwest trending section of the Rhône Valley (between Gletsch and Martigny) marks a major tectonic boundary

between the Helvetic and the Penninic zones of western Switzerland (Fig. 3). Northwest of the Rhône Valley is the Helvetic Zone, dominated by two nappes, the Diablerets and the Wildhorn, which consist of Jurassic and Cretaceous limestones and shales as well as Eocene sandstones. Southeast of the Rhône Valley is the Penninic Zone of western Switzerland, which is composed of Penninic basement nappes and zones of Mesozoic sediments. The Sion-Courmayeur Zone and Combin Zone are belts of Mesozoic sediments, known as Schistes lustrés or Bündnerschiefer, and some ophiolites. The Penninic basement nappes generally include the Gd. St. Bernard, Monte Rosa and Dent Blanche Nappes, which are composed of lithologies such as metasediments and gneisses.

The largest of the Swiss massifs, the Aar Massif, occurs partly within the study area, north of the Rhône Valley (Fig. 3). This crystalline massif underlies the regions of Aletsch Glacier and Bietschhorn. In the Rhône Valley, near Martigny, and in the Mt. Blanc region, two massifs of crystalline basement rocks occur, the Mt. Blanc Massif and the Aiguilles Rouges Massif.

Geologic basis for the ice-surface reconstruction

Most representations of former glacier extents are based on mapping of moraines, which define the geometry of the ablation area. In order to reconstruct the extent of a former glacier above the equilibrium line, in the accumulation area, glacial



Fig. 4. Photos of trimlines in the Grimsel Pass region. The former active ice surface, as interpreted from glacial trimlines, is marked by a dashed white line.

erosional features must be mapped and interpreted. However, the development and preservation of glacial erosional forms, which are etched into bedrock, are highly dependent on the local lithology, structure and weathering characteristics. Therefore, in many areas, these forms are not easily observed or interpreted.

The maximum ice expansion of the last glaciation in Switzerland is well defined on the Alpine forelands by abundant moraines (Jäckli 1962, 1970). The extent of the former ice cap within the inner-Alpine region, the former accumulation area, is less well defined (Favre 1884; Jäckli 1970). We present an ice-surface reconstruction for the accumulation area of the last maximum ice cap in the western Alps. The ice surface is reconstructed based on detailed field mapping of glacial erosional features and periglacial forms and illustrates the ice cap surface geometry and flow lines.

Age of the erosional features

A major assumption, on which the ice-surface reconstruction is based, is that the mapped glacial erosional features were formed by the last maximum ice cap in the Alps. The highest maximum ice surface in the Alps, as marked by erosional features, is correlated with the last maximum extent of ice on the Alpine forelands, as marked by moraines. Radiocarbon and surface exposure dates of moraines show that the last maximum ice extent on the northern Alpine foreland occurred during the last (global) glacial maximum (LGM; ~18,000–20,000 ^{14}C yr BP; Chappell & Shackleton 1986; Schlüchter 1988 and references therein; Ivy-Ochs et al. in press). Therefore, it is assumed that the mapped erosional features are also LGM in age.

Only one other advance of glaciers onto the Alpine forelands extended farther than that during the LGM. The so-called Most Extensive Glaciation (MEG), which covered most of Switzerland and extended as far as Lyon, France, is older than the Penultimate Glaciation, which was approximately 145,000–230,000 yr BP (Schlüchter 1986, 1992). The MEG or other glaciations prior to the LGM may have reached an ice-

surface elevation similar to or higher than the LGM ice cap in the inner-Alpine region (Jäckli 1962). However, due to weathering and erosion in the Alps, glacial erosional features such as striae or polish, formed during glaciations prior to the LGM, would not likely be preserved. For example, using a conservative estimate for erosion in a high relief and mountainous climate of 0.01 mm/year (Press & Siever 1986), a surface formed during the MEG (>230,000 yr BP) would have been eroded by at least 2.3 m. Other erosion rates, in particular for the central Alpine region, are higher (e.g., 0.5 mm/yr; Schlunegger & Hinderer 2003). Over long time periods, even large-scale features such as trimlines would most likely be highly weathered, if not completely erased. Care was taken to attempt to avoid areas that may have been influenced by late-glacial (14,500–10,000 ^{14}C yr BP) or Holocene (10,000 ^{14}C yr BP-present) ice advances. Therefore, research was focused on high ridges and mountain peaks, near the trimline, and outside of late-glacial or Holocene cirques and moraines.

Glacial trimline

The primary erosional feature on which the ice-surface reconstruction is based is the glacial trimline (Fig. 4). A glacial trimline is a boundary on mountain peaks and ridges, below which there is evidence for glacial erosion, such as striae or polish, and above which the bedrock is jagged or frost weathered and does not show evidence of glacial erosion (Thorp 1981; Balantyne 1997). It is assumed that the trimline elevation approximates (within a few tens of meters) the former elevation of the active ice surface.

Glacial trimlines are best preserved on ridges and mountains that are formed of weathering-resistant, massive, crystalline bedrock. Sedimentary and calcareous bedrock types weather more rapidly and glacial erosional forms, such as trimlines, are rarely preserved. Trimlines are also poorly preserved in layered bedrock, or at lithologic or structural contacts. Such layers or contacts may influence weathering and erosion and may erase or mask glacial features.

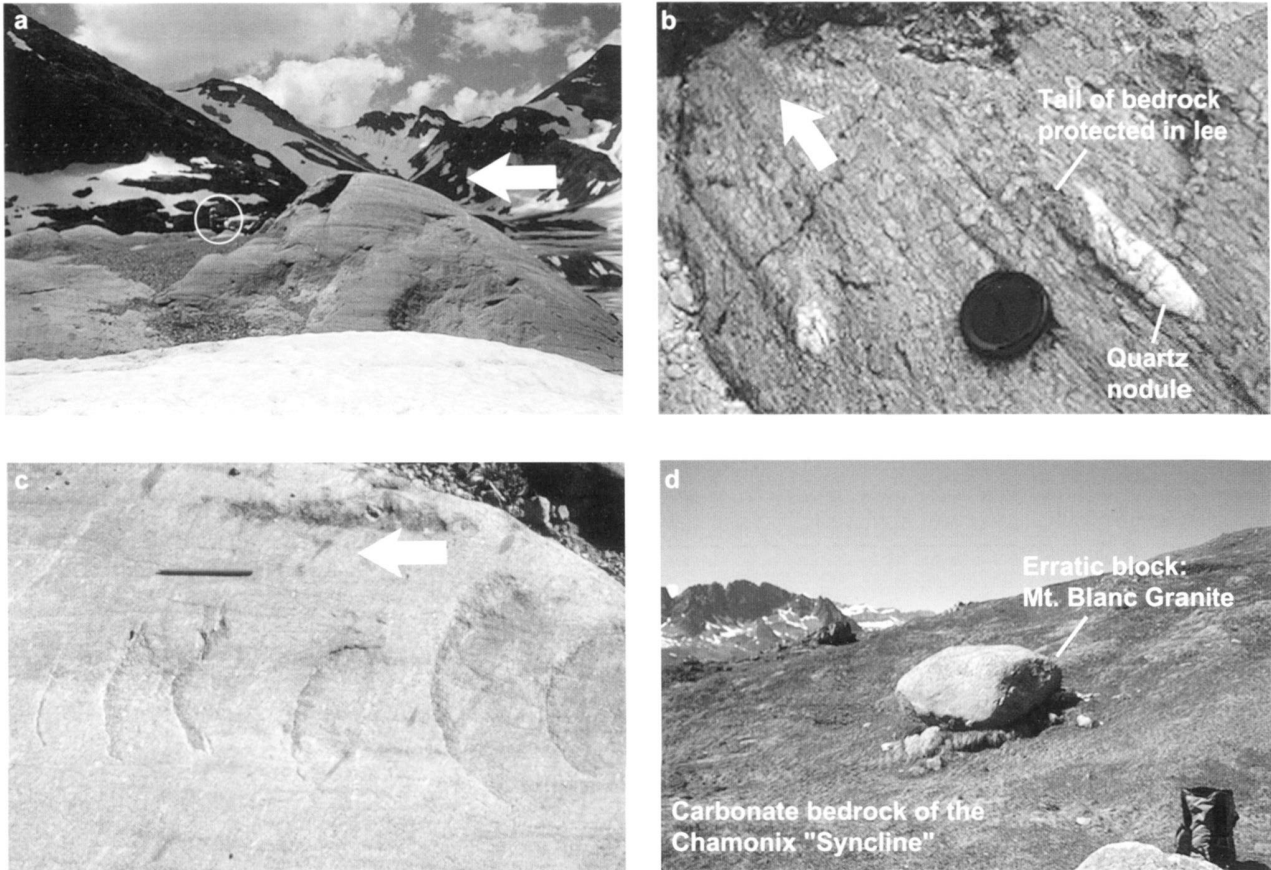


Fig. 5. Photos of glacial erosional features. White arrows show former ice-flow directions. a) Roche moutonnée in the region of Lac d'Emosson. Person marked by white circle for scale. b) Striae and rat tails. c) Friction cracks. d) Erratic block of Mt. Blanc granite located in the Col de Balme.

In an attempt to reduce the likelihood that interpretations of trimline elevations might be influenced by variances in the lithologic or structural features of the bedrock, mapping was conducted in regions where many different bedrock types are present. However, due to physical and chemical properties of certain bedrock lithologies, the extent of a reconstruction based on glacial trimlines is generally limited to regions of metasedimentary and crystalline bedrock types, which are more massive and resistant to weathering. Mapping efforts in the western Alps were focused on regions underlain by the Aar, Mt. Blanc and Aiguilles Rouges Massifs, as well as the metasediments and metavolcanics of the Valpelline complex and the metagranitoids of the Arolla Complex which are part of the Dent Blanche Nappe. Northwest of the Rhône Valley, in the limestone and shale dominated nappes of the Helvetic Zone of western Switzerland, most evidence of ancient glacial erosion has been erased by weathering.

Other erosional features

Smaller scale glacial erosional features provide important additional information for the ice-surface reconstruction, in par-

ticular in regions where glacial trimlines are not well preserved. These features include striae, rat tails, roches moutonnées and friction cracks, and indicate a minimum elevation of the erosive ice surface, as well as former ice flow trends or directions (Chamberlain 1888; Harris 1943; Sugden & John 1976; Laverdière et al. 1985; Benn & Evans 1998; Fig. 5). Erosional features indicating ice-flow directions provide an important check of the ice-surface reconstruction, which is based on trimline elevations. Indicators of ice-flow directions are also necessary to determine the locations of ice domes or diffluentes and to examine ice flow over high-elevation Alpine passes.

Glacial striae are scratches on a bedrock surface produced by clasts embedded in basal ice (Agassiz 1838; Chamberlain 1888; Fig. 5). Striae occur on many different bedrock lithologies but generally are preserved best on fine-grained bedrock types. Striae indicate the general trend, but not the absolute direction, of the former ice flow. A rat tail is a residual ridge of bedrock (10–100 cm length) that exists on the protected, down-ice side of a more resistant rock knob or nodule (Laverdière et al. 1985; Benn & Evans 1998). Based on the location of the residual bedrock, the absolute direction of ice flow is interpreted from a rat tail. Roches moutonnées (<1–100's of meters

length) are asymmetric hills of bedrock that have a molded (up-ice) side and a steep and craggy (down-ice) side (Sugden & John 1976). Small-scale erosional features, such as striae and rat tails, commonly occur on the molded, up-ice side of roches moutonnées.

Friction cracks are crescentic-shaped fractures (10–100 cm length), which dip into a bedrock surface (Fig. 5). They commonly occur as a series of closely spaced fractures (Harris 1943). Two of the most common forms of friction cracks are crescentic gouges and crescentic fractures, both of which indicate the absolute direction of ice flow. Friction cracks generally occur on crystalline, coarse-grained lithologies and may be preserved where other glacial erosional features, such as striae, have been erased by weathering (Harris 1943).

Erratic boulders

Erratic boulders are transported by glacial ice, either as subglacial, englacial or supraglacial clasts, and are composed of a lithology different from the bedrock lithology on which they are deposited (Fig. 5). Indicator erratic boulders are composed of a lithology that has a known and geographically limited origin (Favre 1884). Therefore, based on the origin of an indicator erratic, the flow line along which it was transported can be interpreted. Many erratic boulders occur on the northern and southern Alpine forelands, in the former ablation zone of the LGM ice cap. Some of these boulders are indicator erratics and are important for interpretations of ice-flow directions from the inner-Alpine regions onto the forelands. Erratic boulders also occur in the inner-Alpine regions and are used for the ice-surface reconstruction to indicate a minimum ice-surface elevation and, if possible, ice-flow directions.

Field and GIS mapping

All features were mapped in the field using Swiss 1:25,000 and 1:50,000 topographic maps from the Bundesamt für Landestopographie, French 1:25,000 topographic maps from the Institut Géographique National, and Italian 1:25,000 and 1:30,000 topographic maps from the Istituto Geografico Centrale. The ice-surface reconstruction is based on the Jäckli (1970) ice-surface contour map, updated with 175 points, which represent trimline elevations, and 94 points, which represent other erosional features (elevations and former ice-flow directions; Tab. 1).

The reconstruction is digitally portrayed using the GIS program ArcView. The Jäckli (1970) ice-surface contour map was digitized by Hegner (1995). Trimline and erosional form elevations as well as ice-flow directions were digitized and used to edit the contour lines of the digitized Jäckli (1970) map. A three-dimensional DEM representing the ice surface was created based on the contour lines and data points. The DEM was interpreted using a triangular irregular network (TIN) calculation. A TIN surface is composed of continuous, non-overlapping triangles, which have their edges and points at data lines and data points (ESRI 1997).

In order to compare the three-dimensional ice surface with the land topography, the TIN surface was changed into a grid format. Grids represent three-dimensional surfaces by averaging data points into a mesh of regularly spaced points (ESRI 1997). The grid format allows comparison of two three-dimensional surfaces. RIMINI Höhenmodell 250, a DEM of Switzerland with a grid spacing of 250 m, was used to represent the present land topography (Bundesamt für Landestopographie 2001). Due to the unknown nature of the land topography under the LGM ice cap, it was necessary to use the present land surface for comparison while acknowledging the probability of associated errors. The land-topography grid was subtracted from the ice-surface grid in order to show the representation of ice volume and nunatak areas.

Results: description of the LGM ice surface

The LGM ice cap in the western Alps was characterized by transection glaciers, defined as an interconnected system of valley glaciers (Benn & Evans 1998). These transection glaciers were influenced by at least four main centers of ice accumulation: the Rhône ice dome, the Aletsch icefield, the southern Valais icefield and the Mt. Blanc region (Fig. 6). The main component of the LGM transection glaciers in the western Alps was the glacier in the Rhône Valley, hereinafter referred to as the Rhône Valley Glacier. Numerous ice confluences existed as ice generally followed the preexisting valleys, most of which drained into the Rhône, Arve or Aosta Valleys. At least three major ice diffuences existed: north of Simplon Pass, on Gd. St. Bernard Pass and north of present-day Glacier d'Argentiere. The locations of ice confluences and diffuences were influenced by centers of ice accumulation, such as ice domes and icefields, as well as by the underlying topography.

The Goms

The LGM Rhône ice dome existed at the headwaters of the Rhône Valley, in the central Swiss Alps, and influenced ice flow to the north over Grimsel Pass, to the northeast over Furka Pass, and to the southwest down the Rhône Valley (Florineth and Schlüchter 1998). The Rhône ice dome had a surface elevation of about 2800 m near the present-day Rhône Glacier (Florineth & Schlüchter 1998). Ice flow in the Goms generally followed the valley system and the ice surface sloped down to the southwest, from the Rhône ice dome to 2660 m on Risihorn, north-northeast of Fieschertal.

South of the Goms, the Binntal region was filled with ice to at least 2600 m elevation (Arn 1998). Trimlines in the Binntal region are not obvious due to the predominantly Bündnerschiefer bedrock. However, two passes show evidence of ice spilling out of the Binntal catchment area from north to south. On Albrun Pass (2409 m), which is underlain by augen gneiss, rough roche moutonnée forms indicate ice flow over the pass from northwest to southeast (Arn 1998). Arn (1998) also notes that bedrock ridges above Albrun Pass are more frost-weathered.

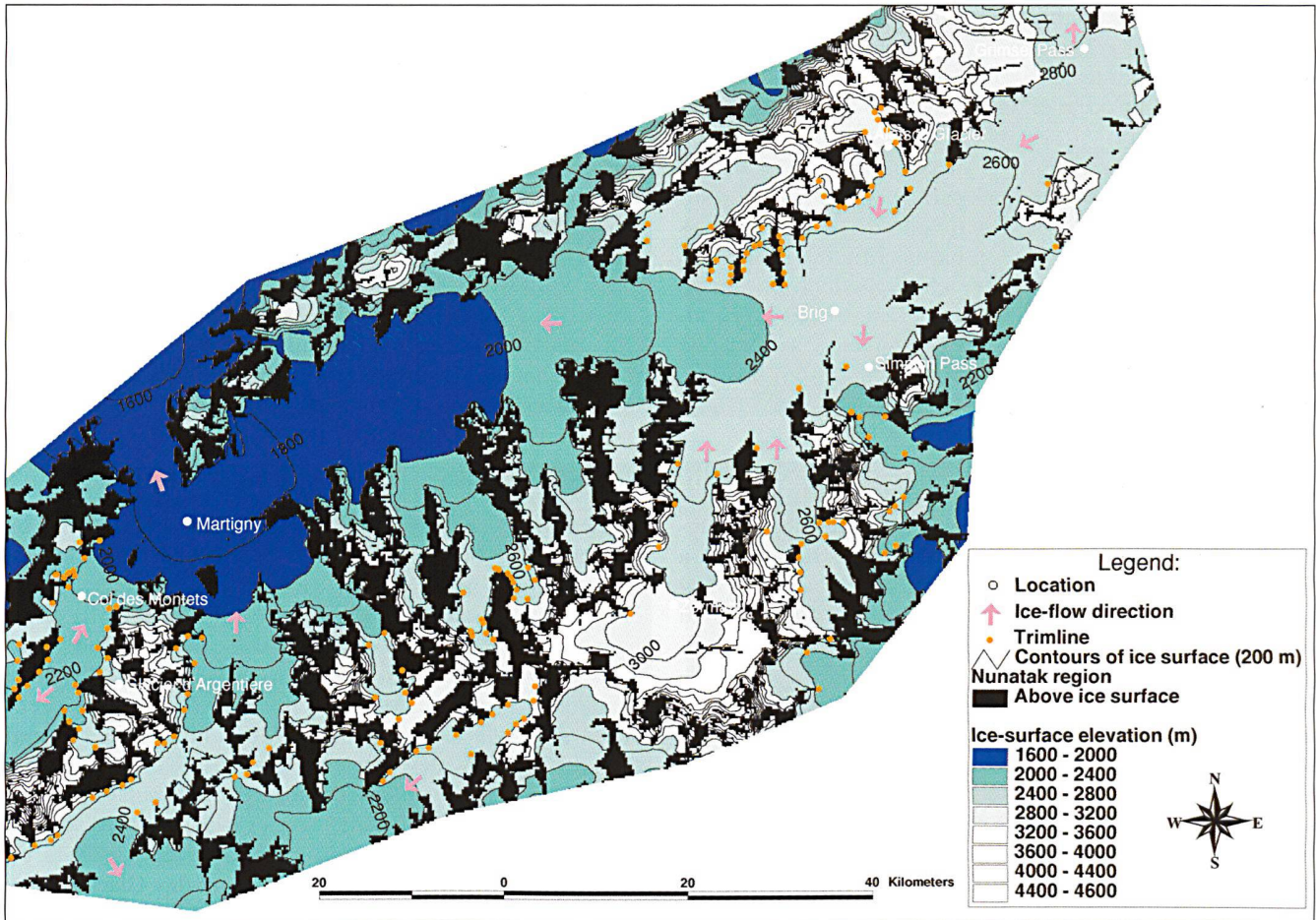


Fig. 6. LGM ice-surface reconstruction, western Swiss Alps and contiguous Alpine regions in France and Italy. For location of the reconstruction see Figs. 1 and 2. The ice-surface elevation is shown as the colored area. Black regions are nunataks. Contour interval is 200 m.

ered at elevations higher than 2600–2700 m. Therefore, it is assumed that the ice thickness on the pass was as much as 200–300 m. Geisspfad Pass (2498 m), underlain by ultramafic bedrock, shows well-developed roches moutonnées and striations, as well as erratic boulders of gneissic composition, all of which indicate ice flow from north to south. A vertical transition to more-weathered bedrock is apparent on the nearby Grampielhorn at approximately 2620 m elevation.

Aletsch icefield

The present-day Aletsch Glacier region was a large icefield that fed into the Rhône Valley Glacier during the LGM. Glacial erosional features in the Aletsch icefield region are well developed and preserved because of the underlying massive and weathering-resistant Aar Massif (Labhart 1977). Trimline elevations can be defined to within a few tens of meters on most bedrock ridges adjacent to the present-day Aletsch Glacier and in the northern ends of Baltschiederental and Bietschtal, which also are underlain by the Aar Massif.

The LGM ice surface was about 2900 m at Konkordiaplatz and sloped down to the south, where it joined the Rhône Valley Glacier at about 2600 m elevation. Ice from the Aletsch region entered the Rhône Valley Glacier through the present Massa River drainage system, as well as through the Märjensee area into Fieschertal. Eggishorn (2927 m) existed as a nunatak, inundated with ice as high as 2680 m. Striations on the bedrock ridge southwest of Bettmerhorn indicate that ice flowed over this ridge, due south, into the Rhône Valley.

Well-developed trimlines in the northern ends of Baltschiederental and Bietschtal are evidence for ice filling these valleys as high as 2850 m. The ice surface in Baltschiederental and Bietschtal sloped down to the south and joined the Rhône Valley Glacier at approximately 2400 m.

Simplon Pass

Simplon Pass (2040 m), south of Brig, is one of the major Alpine passes from the Rhône Valley into Italy (Fig. 7). The bedrock in the pass region, pre-Triassic crystalline basement

rocks, such as mica-schists and gneisses, does not show well-developed trimlines. However, an estimation of the minimum level of the LGM ice surface is made based upon the presence of smaller-scale erosional features.

North-northwest of the pass, striations and rat tails (180°) commonly occur on the southern side of Staldhorn, as well as sparsely on Staldhorn (2462 m) and on the ridge between Staldhorn and Tochuhorn (2648 m) (Fig. 7). Striations and rat tails indicate that Simplon Pass and Staldhorn were covered by ice, which flowed from north to south. Ice-molded forms are also observed on the eastern flank of Tochuhorn at least as high as 2500 m. The ice-erosional features indicate that, during the LGM, ice exited the Rhône Valley Glacier to the south over Simplon Pass, and had a thickness of at least 500 m on the pass. Therefore, an ice diffluence was located in the Rhône Valley, north of Simplon Pass. This ice diffluence marked the separation of ice, which flowed west down the Rhône Valley, from ice that flowed south over Simplon Pass. Ice that flowed over the pass contributed to the Toce/Ticino Glacier drainage system.

Within Simplon Pass, a glaciated landscape is evidenced by numerous ice-erosional forms. Many features, such as rat tails, striae, and grooves, as well as morainic deposits, which exist as high as approximately 2200 m, were attributed to the late-glacial ice advance of the Gondo Stadium (within the Oldest Dryas chron; Müller 1984). The Oldest Dryas chron is the late-glacial time period between the end of the LGM and approximately 13,000 ^{14}C yr BP (Mangerud et al. 1974). During the Gondo Stadium, Chaltwasser and Hohmattu Glaciers flowed to the north, and glaciers, such as Hübsch, Sirwolte, and Rossbode, flowed to the south (Müller 1984). Moraines of smaller late-glacial ice readvances, such as those formed during the Zwischbergen or Dorf Stadiums (within the Oldest Dryas chron), also are preserved within the pass at large (Müller 1984). Features that are attributed to erosion by LGM ice flow are restricted to elevations above 2200 m (Fig. 7). These features are also sparser and more weathered than late-glacial erosional forms.

Southern Valais icefield

The main accumulation area, which fed into the LGM Rhône Valley Glacier, existed in the southern Valais. North-trending valleys, which extend from the Valaisian Alps into the Rhône Valley, as well as west- and south-trending Valpelline and Val Tournche, in Italy, were the locations of the highest regions of the LGM ice cap. The main north-trending valleys include Mattertal, Saastal, Val d'Hérens, Val d'Héremence and Val de Bagnes. The southern Valais icefield had its high-elevation center at the southern end of Mattertal. In the Zermatt region, a large icefield filled the valley to at least 3010 m elevation. Ice flowed outward from this central high region as transection glaciers generally following the pre-existing valleys.

Within Saastal, evidence of ice filling the valley is preserved as trimlines as well as numerous roches moutonnées,

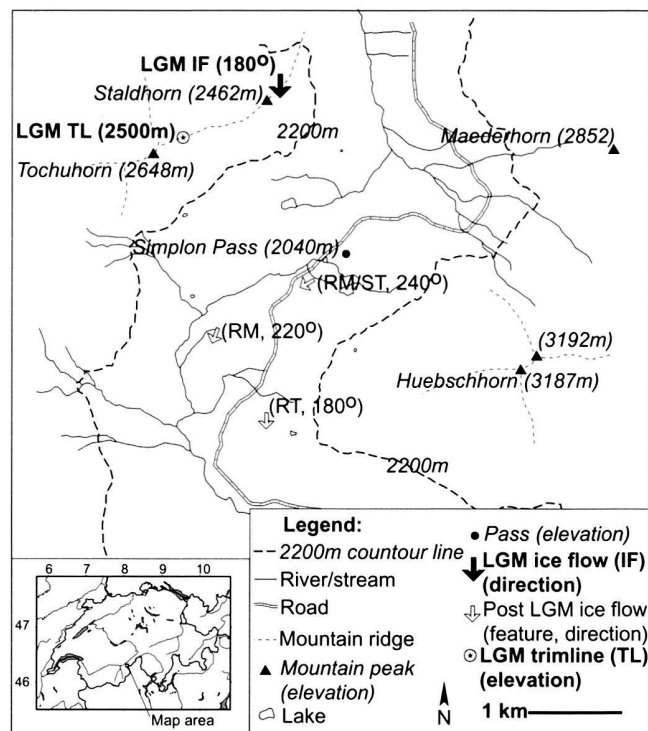


Fig. 7. Detailed map of Simplon Pass. The LGM ice flow (IF) direction and trimline (TL) are shown near Staldhorn. Also shown are erosional features below 2200 m, which are attributed to late-glacial readvances (e.g., Müller, 1984). Mapped ice-flow indicators include roches moutonnées (RM), striae (ST), and rat tails (RT).

striae and polish on the valley walls. Trimlines are best preserved on the valley walls south of Saas Grund, where the underlying bedrock is weathering-resistant crystalline of the Monte Rosa Nappe and the Bernhard Nappe Complex (Bearth 1954). In the region of Saas Grund, the LGM ice surface was as high as 2640 m (west flank of Trifthorn). In the Saas Fee basin, a trimline on the Gulgen shows that the peak was inundated with ice as high as 2900 m. At the southern end of Saastal, in the region of the present-day Mattmark Stausee, the LGM ice surface reached an elevation of at least 2800 m.

Monte Moro Pass (2853 m), at the southern end of Saastal, on the border between Switzerland and Italy, shows erosional features which are most likely younger than the LGM. Roches moutonnées on the northern and southern sides of the pass indicate ice flow to the north and the south, respectively. Such erosional forms suggest that the pass, at one time, was an ice diffluence. However, due to the close proximity (<1 km) of present-day glaciers, it is likely that these features were formed during late-glacial ice advances.

Trimlines in Mattertal are not well developed because of the variable and weathering-susceptible bedrock lithologies. However, between Zermatt and the high mountain ridge to the south, glacial striae on the Gornergrat provide evidence of a large LGM icefield, which had a surface elevation at least as

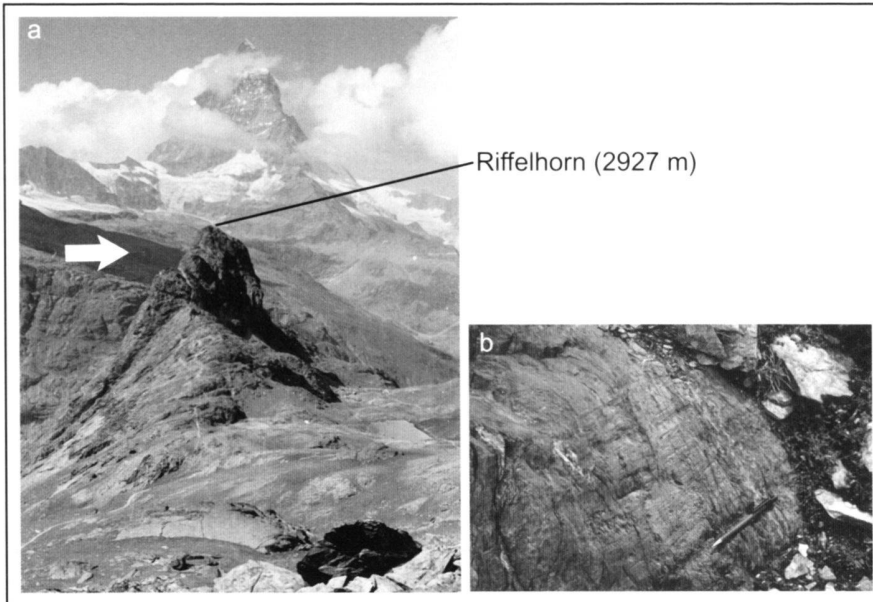


Fig. 8. Photos of the Gornergrat near Zermatt, southern Valais. a) Photo of the Riffelhorn (2927 m elevation), which shows roche moutonnée forms. The Riffelhorn was completely covered by ice flowing from left to right (to the north). b) Photo of striations on the Gornergrat, at 3010 m elevation.

high as 3010 m (Fig. 8). West of Gornergrat train station, these striae exist in at least 15 locations, some of which are as high as 3010 m elevation, and trend northwest ($320\text{--}330^\circ$). The glacial striae are etched into the ultramafic bedrock and occur only as small patches that have been protected from weathering. The morphologic form of Riffelhorn (2927 m), west of Gornergrat train station, also shows that it has been overrun by ice and its rock walls preserve abundant glacial polish and striae (Fig. 8). Such evidence indicates that erosive ice overflowed Gornergrat from southeast to northwest and that the active ice surface was at least as high as 3010 m.

The well-developed glacial trimlines in Valpelline, southeast of Matternal, also show that a large glacier filled the valley during the LGM. Trimlines in the northern end of Valpelline are as high as 2900 m near the Tête des Roëses. The LGM ice surface sloped down to the southwest and was approximately 2580 m near the mouth of the valley. Although the ice surface was at a high elevation (at least 2900–3000 m) in the southern Valais, the high mountain ridges of the Dent d'Hérens, Matterhorn, Breithorn and Monte Rosa contained the ice flow generally to within the pre-existing valley systems.

Gd. St. Bernard Pass

Trimlines in the Gd. St. Bernard Pass region are not obvious but some, including a trimline (2650 m) east of the pass on Mt. Mort, are evident. Well-developed glacial erosional features are prevalent on the northeastern side of Gd. St. Bernard Pass between the Hospice and the northern portal of the Gd. St. Bernard tunnel (Fig. 9). Erosional features in this area include numerous roches moutonnées, large (~20 cm diameter) rat tails, as well as abundant striated and polished surfaces. At the pass (2470 m), striae and rat tails show ice flow to the north-

east (50°), whereas northeast of the pass such forms indicate ice flow trending to the north ($2375\text{ m}, 30^\circ$ and $2300\text{ m}, 10^\circ$). The change in the trend of striae and rat tails generally follows the trend of the Val d'Entremont, therefore indicating a strong influence of the underlying topography on the ice-flow directions.

Striae and a few small rat tails occur on the west side of the lake that is located at the pass ($2470\text{ m}, 265^\circ$). These features indicate ice flow to the west from the pass. Based on ice-flow directions both to the northeast and to the west of the pass, as indicated by erosional forms, the pass was an ice diffluence. Strongly erosive ice flow is much more evident on the northeastern side of the pass and into the Val d'Entremont than on the southern side of the pass.

Mt. Blanc region

The LGM ice-surface elevation on the French side of the Mt. Blanc region was mapped in cooperation with Sylvain Couterand. The LGM reconstruction on the Italian side of Mt. Blanc is based on field mapping and on trimline elevations from Porter & Orombelli (1982).

On the north side of the Mt. Blanc region, the LGM ice surface in the Chamonix Valley was highest (2200–2300 m) near the present-day Glacier d'Argentière. This high elevation region was the location of an ice diffluence. Striations and rat tails on L'Aiguillette des Posettes ($340^\circ, 2201\text{ m}$) and within the Col des Montets (1461 m) show that, during the LGM, ice flowed to the north. Ice east of the diffluence flowed over the Col du Balme and Col des Montets and was joined by ice from catchment areas near the Lakes of Emosson and the present-day Trient Glacier. This ice then entered the Rhône Valley Glacier between Martigny and Vernayaz. West of the Glacier

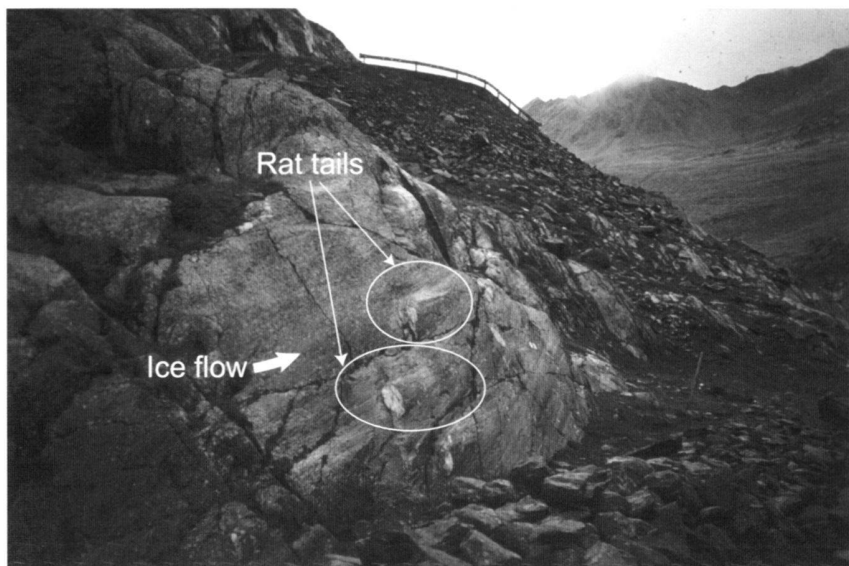


Fig. 9. Rat tails on the northeastern side of Gd. St. Bernard Pass (head of Val d'Entremont.) The large rat tails show strongly erosive ice flow from left to right (to the northeast).

d'Argentière ice difffluence, ice flowed to the southwest, down the Chamonix Valley and joined the Arve Glacier.

On the Italian side, ice flowed out from the high peaks of the Mt. Blanc Massif into Val Veny and Val Ferret. In these valleys, the maximum ice surface was as high as 2600 m. Ice from Val Veny and Val Ferret overtopped Mt. Chetif (2343 m), near Entrèves, and followed the Dora Báltea drainage system. Some ice may have spilled out of Val Ferret to the northeast, over the Petit Col du Ferret (2490 m) and into the Rhône Valley Glacier. Glacial erosional features are not present in the Petit Col du Ferret because of the highly weathered bedrock of the Courmayeur-Sion Zone. However, the LGM ice-surface elevation, as evidenced by trimlines on the ridges south of Mont Dolent and Aiguille de Triolet (~2750 m), indicates that ice must have overtopped the col.

Interpretations

The LGM ice cap in the western Alps: transection glaciers

By definition, transection glaciers occur in mountain landscapes that are "too dissected to support an ice cap" and where ice is evacuated too effectively to "produce a dome-like profile" (Benn & Evans 1998, p.19). The transection glaciers in the western Alps were influenced by large relief of the land topography which dissected the ice. However, these transection glaciers were also characterized by numerous ice confluences and by deep and narrow valleys (*e.g.* the Rhône Valley between Martigny and Bex is < 2 km wide and ~1000 m below the present valley floor; Pfiffner et al. 1997) which would contribute to inefficient evacuation of ice.

Except for the LGM Rhône ice dome, located at the head of the Rhône Valley, the main centers of LGM ice accumulation that influenced the transection glaciers in the western

Alps, in particular in the southern Valais, Aletsch and Mt. Blanc regions, were characterized by icefields instead of ice domes. In these regions, the high-elevation mountain peaks and ridges and low elevation valleys most likely dissected the ice to an extent that prevented the formation of ice domes. For example, the LGM southern Valais icefield had a surface elevation of at least 3010 m and was at least 1400 m thick in the Zermatt region. These dimensions are similar to those of the large Engadine ice dome in the eastern Swiss Alps (Florineth & Schlüchter 1998). However, the southern Valais is characterized by some of the largest relief in Switzerland (2000–3000 m; Kühni & Pfiffner 2001). Although the LGM ice thickness in the Zermatt region was >1000 m, an ice dome did not exist because the ice was dissected by mountain ridges and ice flow was confined to follow the pre-existing topography.

Ice from the Aletsch icefield flowed south and entered the Rhône Valley Glacier at Brig. The floor of the glacially shaped Massa Valley mouth, north of Brig, is approximately 200 m higher than the present valley floor in Brig (Hantke 1980). Therefore, at this confluence, ice from the Aletsch region must have entered the Rhône Valley Glacier with a steep longitudinal profile and at an approximate right angle. The Rhône Valley east of Brig shows a wide basin that is most apparent as a half-circle form carved out of the south valley wall, which is composed of Bündnerschiefer bedrock (Burri et al. 1993; Hantke 1980). We suggest that the steep and southward flowing ice from the Aletsch icefield influenced the Rhône Valley Glacier such that the southern valley wall was eroded and ice from the Rhône Valley Glacier, and also possibly from the Aletsch region, was forced over Simplon Pass. Studies of indicator erratic boulders south of Simplon Pass are necessary to investigate this hypothesis.

A confluence between ice from the Mt. Blanc region and the Rhône Valley Glacier existed near Martigny (Fig. 6). From

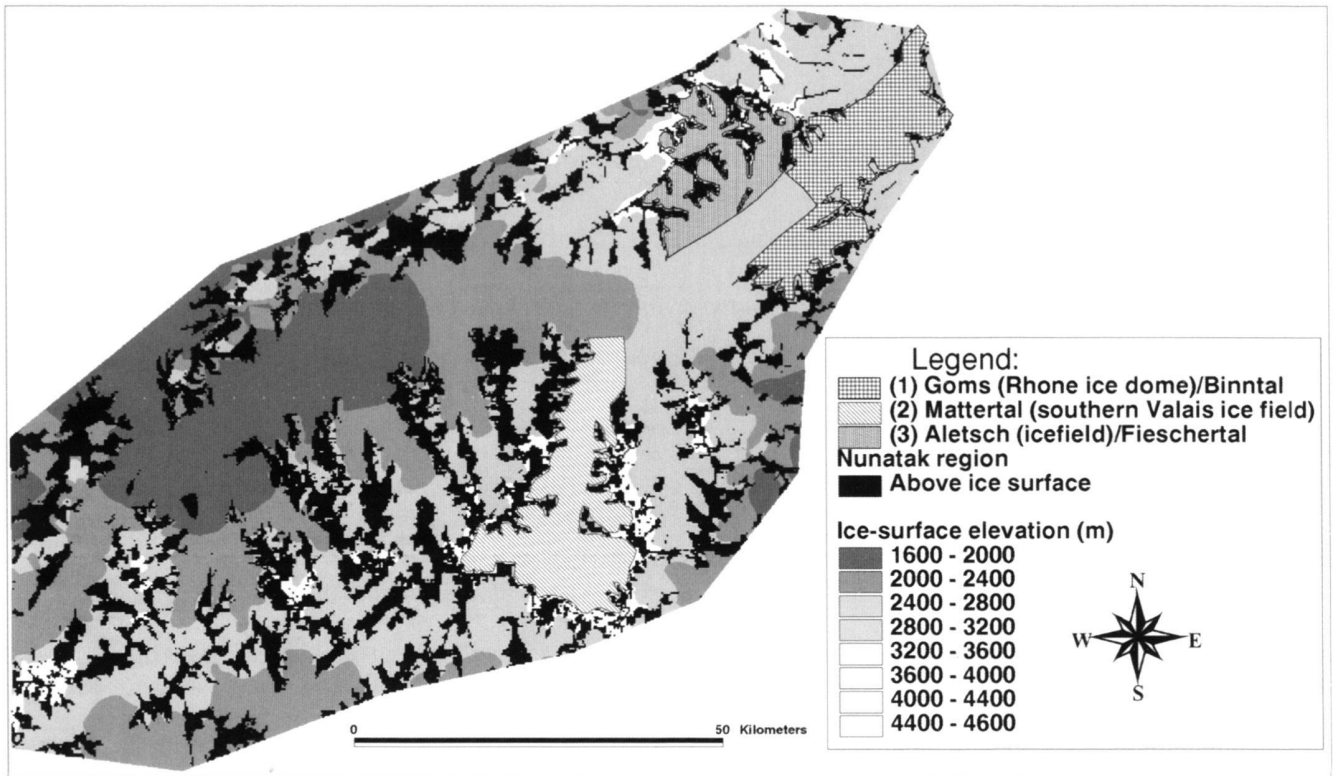


Fig. 10. Outline of 1) Goms (Rhône ice dome)/Binntal, 2) Mattertal (southern Valais icefield) and 3) Aletsch (icefield)/Fieschertal, where the LGM ice volumes are calculated based on the reconstructed LGM ice surface and the present day topography, as represented by RIMINI.

the ice diffuence north of present-day Glacier d'Argentière, ice flowed northeast, over the Col des Montets and the Col de Balme. The LGM ice surface in Martigny was approximately at 1800 m elevation. Seismic studies indicate that the bedrock floor of the Rhône Valley at Martigny is approximately 1000 m below the present valley floor (Pfiffner et al. 1997). It is hypothesized that the valley-fill near Martigny consists of LGM till and post-LGM meltwater and lacustrine deposits (Pfiffner et al. 1997). Therefore, the LGM ice thickness near Martigny may have been as much as 2300 m.

LGM ice volumes in selected regions

Between the Goms and Sion, the Rhône Valley Glacier was influenced by the Rhône ice dome and at least two main centers of ice accumulation, the Aletsch and southern Valais icefields (Fig. 6). The LGM ice-surface areas and ice volumes for the regions of 1) the Goms (Rhône ice dome)/Binntal, 2) Mattertal (southern Valais icefield) and 3) the Aletsch (icefield)/Fieschertal, are estimated based on the reconstructed LGM ice surface and the present-day land topography as represented by RIMINI (Fig. 10). Ice-volume estimates are subject to the uncertainty of assuming that the present-day topography is the same as the LGM land topography. Nevertheless, the results show that the LGM ice volume in the Goms/Binntal (170 km^3)

was similar to that in Mattertal (170 km^3) (Fig. 10). Ice in the Goms/Binntal drained through at least six outlets, partially contributing ice to the Rhône Valley Glacier, but also exiting the Rhône Valley over the Grimsel, Furka, Nufenen, Albrun and Geisspfad Passes (Florineth & Schlüchter 1998). In comparison, ice in Mattertal drained through only one outlet, down Vispental and into the Rhône Valley, thus contributing the total calculated ice volume to the Rhône Valley Glacier.

Based on the calculated LGM ice volume for Mattertal, which constituted only part of the total ice in Vispental, we suggest that ice from Vispental dominated ice flow in the Rhône Valley west of Visp. The large ice input from the southern Valais icefield may have forced the Rhône Valley Glacier northward or dammed ice flow in the Rhône Valley to the east/northeast of Visp. Additional ice from tributary valley glaciers such as Turtmantal, Val de Zinal, Val d'Hérens, Val d'Héremence, Val de Bagnes and Val d'Entremont also contributed to the Rhône Valley Glacier and continually pushed ice to the northern side of the Rhône Valley.

The total calculated LGM ice volume for the Aletsch (icefield)/Fieschertal (50 km^3) (Fig 10.) is subject to a substantial adjustment because the land topography as portrayed by RIMINI includes the present day glacier surfaces. Thus, the volumes of present day Aletsch and Fiescher Glaciers must be added to the calculated LGM ice volume for the Aletsch (ice-

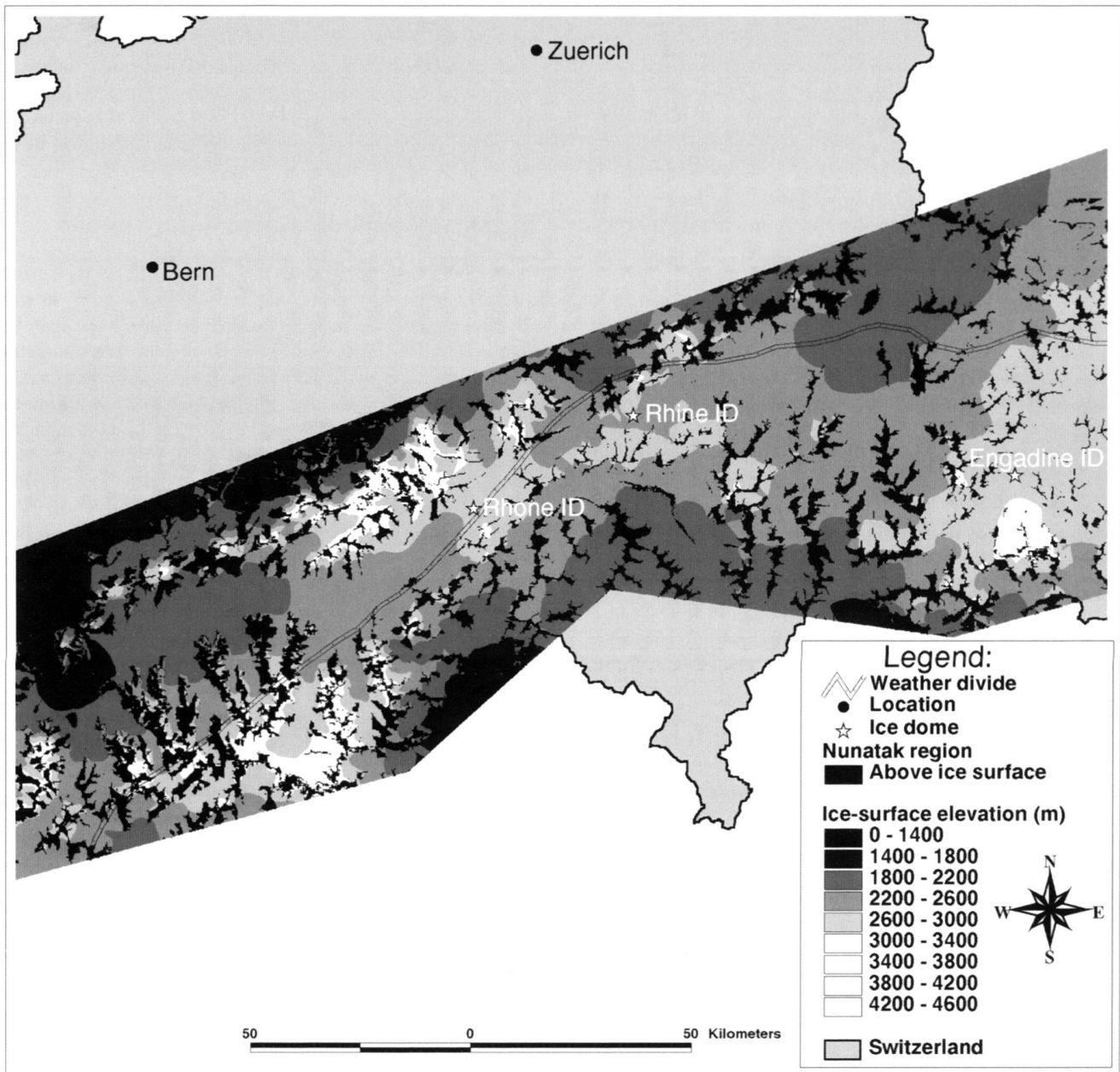


Fig. 11. Ice-surface reconstruction, Swiss Alps. The ice-surface elevation is shown in white and shades of gray. Black regions are nunataks. Also shown is the present weather divide, according to Fliri (1984). Data from the eastern and central Swiss Alps, including the locations of ice domes (ID), are from Florineth & Schlüchter (1998, 2000).

field)/Fieschertal in order to represent a more accurate LGM ice volume estimate.

Distribution of erratic boulders on the northern Alpine foreland

During the LGM, the Rhône Valley Glacier extended onto the northern Alpine foreland as a large piedmont glacier, known

as Rhône Glacier. Restricted by the Jura Mountains, Rhône Glacier split into two lobes: one lobe flowed west into the Lake Geneva basin and one, the Solothurn Lobe, flowed east-northeast and terminated at Wangen a.A. (de Charpentier 1841; Jäckli 1962, 1970; Hantke 1980; Fig. 1). The distribution of erratic boulders (some as large as >100 m³) on the northern Alpine foreland, in particular those transported by the Solothurn Lobe, indicates that ice flow in the Rhône Valley

was complex (Hantke 1980). For example, boulders of lithologies such as Hornblende Granite (arkesine) and Smaragdit Gabbro, which originate in Saastal, occur on Rhône Glacier end moraines between Biel and Wangen a.A. (Hantke 1980). Boulders of Vallorcine Conglomerate exist on the former right lateral margin of the Solothurn Lobe, between Grauholz and Hindelbank. Other boulders from the southern Valais and the Mt. Blanc region, including Mt. Blanc Granite, were also transported and deposited by the Solothurn Lobe, for example in the Seeland region of the northern Alpine foreland (Hantke 1978).

The LGM ice-surface reconstruction and estimates of LGM ice volume for selected regions presented in this paper suggest a mechanism by which boulders from the southern Valais, and possibly from the Mt. Blanc region, were transported to the Solothurn Lobe of the Rhône Glacier. As discussed above, ice from the southern Valais icefield dominated ice flow in the Rhône Valley west of Visp, possibly forcing the Rhône Valley Glacier to the northern side of the valley, or damming the Rhône Valley Glacier to the east/northeast of Visp. Such ice flow would allow for the transport of boulders from the southern Valais between Visp and Vernayaz to the middle or right-lateral side of the Rhône Valley Glacier and to the Solothurn Lobe. It is also possible that the LGM Rhône Valley Glacier experienced unstable (*i.e.*, surging) ice flow. Surging ice-flow may have influenced the contorting of lateral and medial moraines, resulting in the distribution of indicator erratics on the northern Alpine foreland.

It is assumed that indicator erratic boulders present on LGM moraines of the Solothurn Lobe were transported from their origins in the Alps during the LGM. However, it is possible that erratic boulders from the southern Valais and Mt. Blanc regions that occur in the LGM moraines were transported to the northern Alpine foreland during prior glaciations. In this case, erratic boulders on the northern Alpine foreland would have been reworked and re-deposited by the LGM Solothurn Lobe.

LGM ice-surface geometry and paleo-atmospheric circulation

In the eastern and central Swiss Alps, the locations of the Engadine and Rhine ice domes, south of the present weather divide, indicate that the dominant LGM atmospheric circulation pattern was south/southwesterly (Florineth & Schlüchter 1998, 2000) (Fig. 11). The LGM Rhône ice dome, as mapped by Florineth & Schlüchter (1998), was located approximately on the present weather divide and therefore was affected by precipitation related to both (north)westerly and south/southwesterly circulation patterns. However, the direction of ice flow from the Rhône ice dome to the north over the Grimsel Pass is interpreted to reflect an increased contribution of southerly circulation during the LGM (Florineth & Schlüchter 2000).

Notwithstanding the absence of ice domes in the western Alps, one main LGM center of ice accumulation, the southern Valais icefield, also reflects a paleo-atmospheric circulation

pattern that is consistent with the hypothesis reported by Florineth & Schlüchter (1998, 2000). The LGM southern Valais icefield was centered in the Zermatt region which is located south of the present weather divide (Fliri 1984). Therefore, the location of this large icefield also supports a strong influence of south/southwesterly atmospheric circulation in the western Alps during the LGM.

Conclusions

We present a detailed reconstruction of the LGM ice surface in western Swiss Alps and contiguous Alpine regions in Italy and France. The ice-surface reconstruction shows that the LGM accumulation area in the western Alps was characterized by transection glaciers. The high relief of the western Alps dissected the ice surface and confined ice flow to follow the pre-existing valley system. An estimate of LGM ice volumes in three regions, the Goms (Rhône ice dome)/Binntal, the Mattertal (southern Valais icefield) and the Aletsch (icefield)/Fieschertal, indicates that the largest input into the Rhône Valley Glacier was from the southern Valais icefield. The ice flow from the southern Valais icefield, in particular from Vispental, may have been responsible for the transport of erratic boulders from the southern Valais and the Mt. Blanc regions across the Rhône Valley and to the Solothurn Lobe on the northern Alpine foreland. The location of the large southern Valais icefield is consistent with dominant south/southwesterly paleo-atmospheric circulation, as interpreted from the ice-surface geometry in the eastern and central Swiss Alps (Florineth & Schlüchter 2000).

Acknowledgements

This research is part of the Ph.D. thesis of M. Kelly and was supported by Swiss National Science Foundation grant number: 20-65153.01. S. Couterrand provided much of the field data from the Chamonix Valley. M. Gasser provided initial field data in the Aletsch region. E. Pointner is responsible for a special opportunity for the first author to map erosional features from high elevation in the southern Mattertal. Assistance in the field from A. Brandes, J. Daly, A. Hormes, C. Monroe, D. Radies and D. Sanz is appreciated. Comments on the manuscript by D. Kelly and his support in the field greatly improved this work. The authors thank M. Fiebig and D. van Husen for critical and helpful reviews.

REFERENCES

- AGASSIZ, L. 1837: Discours prononcé à l'ouverture des séances de la Soc. helv. sci. natur. à Neuchâtel, le 24 juillet 1837, par L. AGASSIZ, président: Actes Soc. Helv. Sci. Nat., réunie à Neuchâtel, 22. sess., Neuchâtel, 5–32.
- AGASSIZ, L. 1838: On the polished and striated surfaces of the rocks which form the beds of glaciers in the Alps. Proc. geol. Soc. London 3, 321–322.
- ARN, K. 1998: Quartärgeologie im Binntal und in Südchile (41°S). Unpubl. Diploma thesis, Univ. Bern, 116 p.
- BALLANTYNE, C. 1997: Periglacial trimlines in the Scottish Highlands. Quat. Int. 38/39, 119–136.
- BEARTH, P. 1954: Geologischer Atlas der Schweiz 1:25,000, Saas, Blatt 534, Kümmerly and Frey, Bern, Switzerland.
- BECK, P. 1926: Eine Karte der letzten Vergletscherung der Schweizeralpen, 1. Mitt. Naturwiss. Ges., Thun, Switzerland.

- BENN, D.I. & EVANS D.J.A. 1998: *Glaciers and Glaciation*. John Wiley & Sons, Inc., New York, NY, USA, 734 p.
- Bundesamt für Landestopographie 2001: RIMINI Höhenmodell 250 m. Seftigenstrasse 264, Postfach, CH-3084 Wabern.
- BURRI, M., FRANK, E., JEANBOURQUIN, P., LABHART, T., LISZAKY M. & STRECKEISEN, A. 1993: *Geologischer Atlas der Schweiz 1:25.000*, Brig, Blatt 1289, KÜMMERLY and FREY, Bern, Switzerland.
- CAMPY, M. & ARN, R. 1991: The Jura glaciers: paleogeography in the Würmian circum-Alpine zone. *Boreas* 20, 17–27.
- CHAMBERLAIN, T.C. 1888: The rock-scourings of the great ice invasions. *U.S. Geol. Survey, 7th Annual Report*, 155–248.
- CHAPPELL, J. & SHACKLETON, N.J. 1986: Oxygen isotopes and sea level. *Nature* 324, 137–140.
- CLIMAP, P.M. 1976: The surface of the ice age earth. *Science* 191/4232, 1131–1137.
- DE BEAULIEU, J.-L., MONTJUVENT, G. & NICLOUD, G. 1991: Chronology of the Würmian glaciation in the French Alps: A survey and new hypotheses. In: FRENZEL, B. (Ed.): *Klimageschichtliche Probleme der letzten 130 000 Jahre*. Gustav Fischer Verlag, Stuttgart, 435–448.
- DE CHARPENTIER, J. 1841: *Essai sur les glaciers et sur le terrain erratique du bassin du Rhône*. Karte und 8 Abbildungen, Lausanne, Switzerland, 363 p.
- DÉVERIN, L. 1936: *Carte Géotechnique de la Suisse, 1:200,000, Feuille No. 3, Genève–Lausanne–Sion, Texte explicatif*. KÜMMERLY and FREY, Bern, Switzerland, 104 p.
- ESRI 1997: *ArcView 3D Analyst*. Environmental Systems Research Institute, Redlands (California) USA, 118 p.
- ESCHER, A., MASSON, H. & STECK, A. 1993: Nappe geometry in the Western Swiss Alps. *J. Struct. Geol.* 15, 501–509.
- ESCHER, A., HUNZIKER, J.-C., MARTHALER, M., MASSON, H., SARTORI, M. & STECK, A. 1997: Geologic framework and structural evolution of the western Swiss-Italian Alps. In: PFIFFNER, A.O., LEHNER, P., HEITZMANN, P., MUELLER, ST., & STECK, A. (Eds.). *Deep Structure of the Swiss Alps: Results of NRP 20*. Birkhäuser Verlag, Basel, Switzerland, 205–221.
- FAVRE, A. 1884: *Carte des anciens glaciers du versant nord des Alpes suisses, 4 feuilles au 1:250,000*.
- FLURI, F. 1984: *Synoptische Klimatographie der Alpen zwischen Mont Blanc und Hohen Tauern (Schweiz – Tirol – Oberitalien)*. *Wiss. Alpenvereinsh.* Heft 29, 686 p.
- FLORINETH, D. 1998: Surface geometry of the Last Glacial Maximum (LGM) in the southeastern Swiss Alps (Graubünden) and its paleoclimatological significance. *Eiszeitalter u. Gegenwart* 48, 23–37.
- FLORINETH, D. & SCHLÜCHTER CH., 1998: Reconstructing the Last Glacial Maximum (LGM) ice surface geometry and flowlines in the Central Swiss Alps. *Eclogae Geol. Helv.* 91, 391–407.
- 2000: Alpine evidence for atmospheric circulation patterns during the Last Glacial Maximum. *Quaternary Research* 54, 295–308.
- FREI, R. 1912: *Monographie des Schweizerischen Deckenschotter*. *Beitr. Geol. Karte Schweiz, NF.* 37.
- HAEBERLI, W. 1976: *Eistemperaturen in den Alpen*. *Z. Gletscherkde. Glazialgeol.*, 11, 203–220.
- HAEBERLI, W. & PENZ, U. 1985: An attempt to reconstruct glaciological and climatological characteristics of 18 ka BP ice age glaciers in and around the Swiss Alps. *Z. Gletscherkde. Glazialgeol.* 21, 351–361.
- HANTKE, R. 1978: *Eiszeitalter. Band 1*, Ott Verlag, Thun, Switzerland, 469 p.
- 1980: *Eiszeitalter. Band 2*, Ott Verlag, Thun, Switzerland, 703 p.
- HARRIS, S.E. 1943: Friction cracks and the direction of glacier movement: *J. Geol.* 51, 244–258.
- HEGNER, J.M. 1995: *Die Schweiz zur letzten Eiszeit. Eine digitale Bearbeitung*. Diploma thesis, ETH Zürich, 54 p.
- IVY-OCHS, S., SCHÄFER, J., KUBIK, P.W., SYNAL, H.-A. & SCHLÜCHTER, CH. in press: *Deglaciation timing on the northern Alpine foreland (Switzerland)*. *Eclogae Geol. Helv.*
- JÄCKLI, H. 1962: *Die Vergletscherung der Schweiz im Würmmaximum*. *Eclogae geol. Helv.* 55/2, 285–294.
- 1970: *Die Schweiz zur letzten Eiszeit, Karte 1:550 000. Atlas der Schweiz, Blatt 6*, Bundesamt für Landestopographie, Wabern–Bern, Switzerland.
- KÜHNI, A. & PFIFFNER, A.O. 2001: The relief of the Swiss Alps and adjacent areas and its relation to lithology and structure: topographic analysis from a 250-m DEM. *Geomorphology* 41, 285–307.
- LABHART, T.P. 1977: *Aarmassiv und Gottardmassiv*. In: GWINNER, M.P. (Ed.): *Sammlung geologischer Führer Bd. 63, Gebrüder Bornträger, Berlin/Stuttgart*, 173.
- LAVERDIÈRE, C., GUIMONT, P. & DIONNE, J.-C. 1985: Les formes et les marques de l'érosion glaciaire du plancher rocheux: signification, terminologie, illustration. *Palaeogeography, Palaeoclimatology, Palaeoecology* 51, 365–387.
- MAISCH, M., WIPF, A., BERNHARD, D., BATTAGLIA, J. & BENZ, C. 2000: *Die Gletscher der Schweizer Alpen*. Hochschulverlag, ETH Zürich, Switzerland, 373 p.
- MANGERUD, J., ANDERSEN, S.T., BERGLAND, B.E. & DONNER, J.J. 1974: Quaternary stratigraphy of Norden, a proposal for terminology and classification. *Boreas* 3, 109–126.
- MÜLLER, H.-N. 1984: *Spätglaziale Gletscherschwankungen in den Westlichen Schweizer Alpen und im Nordisländischen Tröllaskagi-Gebirge*. Buchdruckerei Küng, Näfels, Switzerland, 205 p.
- PENCK, A. & BRÜCKNER, E. 1909: *Die Alpen im Eiszeitalter*. *Tauchnitz, Leipzig*, 1199 p.
- PFIFFNER, A.O., HEITZMANN, P., LEHNER, P., FREI, P., PUGIN, A. & FELBER, M. 1997: Incision and backfilling of Alpine Valleys: Pliocene, Pleistocene and Holocene processes. In: PFIFFNER, A.O., LEHNER, P., HEITZMANN, P., MUELLER, ST. & STECK, A. (Eds.): *Deep Structure of the Swiss Alps: Results of NRP 20*. Birkhäuser Verlag, Basel, Switzerland, 265–288.
- PORTER, S.C. & OROMBELLI, G. 1982: Late-glacial ice advances in the western Italian Alps. *Boreas* 11, 125–140.
- PRESS, F. & SIEVER, R. 1986: *Earth*. W.H. FREEMAN and Company, New York, 656 p.
- SCHLÜCHTER, C. 1986: *The Quaternary Glaciations of Switzerland, with special reference to the northern alpine foreland: Final Report of the IGCP–Project 24 Quaternary Glaciations of the Northern Hemisphere*. *Quat. Sci. Rev.* 5, 413–419.
- 1988: The deglaciation of the Swiss-Alps: A paleoclimate event with chronological problems. *Bull. Ass. Franç. étude du Quaternaire* 2/3, 141–145.
- 1992: *Terrestrial Quaternary Stratigraphy*. *Quat. Sci. Rev.* 11, 603–607.
- SCHÜEPP, M. 1965: *Klima und Wetter I: Atlas der Schweiz*. Eidg. Landes-topographie, Wabern–Bern, Switzerland.
- SCHLUNEGGER, F. & HINDERER, M. 2003: Pleistocene/Holocene climate change, re-establishment of fluvial drainage network and increase in relief in the Swiss Alps. *Terra Nova* 15/2, 88–95.
- SUGDEN, D.E. & JOHN, B.S. 1976: *Glaciers and Landscape: A Geomorphological Approach*. EDWARD ARNOLD, London, 376 p.
- THORP, P.W. 1981: A trimline method for defining the upper limit of the Loch Lomond Advance glaciers: examples from the Koch Levan and Glencoe areas. *Scot. J. Geol.* 17, 49–64.
- TRÜMPY, R. 1980a: *Geology of Switzerland, A Guide-Book, Part A: An Outline of the Geology of Switzerland* (Ed. by Schweizerische Geologische Kommission). Wepf and Co. Publishers, Basel and New York, 104 p.
- 1980b: *Geology of Switzerland, A Guide-Book, Part B: Geological Exkursions* (Ed. by Schweizerische Geologische Kommission). WEPF and Co. Publishers, Basel and New York, 334 p.
- VAN HUSEN, D. 1987: *Die Ostalpen in den Eiszeiten*. *Geologische Bundesanstalt Österreichs, Wien*, 24 p.
- VENETZ, I. 1822: *Sur les variations du climat dans les Alpes*. *Bibl. Univ. Sci. Genève*, 21.
- 1829: *Mémoire sur l'extension qu'il présume que les glaciers avaient autrefois*. *Verh. Schweiz. Natf. Ges.* 15, 31.
- WIDMANN, M. & SCHÄR, C. 1997: A principal component and long-term trend analysis of daily precipitation in Switzerland. *Int. J. Climat.* 17, 1333–1356.

Manuscript received January 24, 2003

Revision accepted December 9, 2003

Tab. 1. List of trimline elevations (z) used as the basis of the LGM ice-surface reconstruction. Locations are described by the x- and y-coordinates of the Swiss map system.

TL-ID	LOCATION	X-COORD	Y-COORD	Elevation (Z)	MAP_#	MAP_NAME
1	Schwarzhorn	622350	138725	2600	1268	Loetschental
2	Alplijhorn	622225	136975	2550	1268	Loetschental
3	Hogleifa	626325	136400	2540	1268	Loetschental
4	Bietschhornhutte	629200	138425	2580	1268	Loetschental
5	Jegihorn	629775	134850	2600	1268	Loetschental
6	Crutighorn	631350	134075	2600	1268	Loetschental
7	Jaegihorn (Baltschiederklause)	634700	138375	2850	1268	Loetschental
8	Stockhorn(SE)	634450	136625	2640	1268	Loetschental
9	Stockhorn(S)	633875	136350	2660	1268	Loetschental
10	Tieregghorn	633075	135600	2600	1268	Loetschental
11	Dubihorn	632700	134775	2600	1268	Loetschental
12	Gruebhorn	636550	137450	2800	1268	Loetschental
13	Strahlhorn	636825	136825	2700	1268	Loetschental
14	Laegundegrat (Gredetsch)	636650	136075	2640	1268	Loetschental
15	Alpjuhorn (E)	636900	135450	2600	1268	Loetschental
16	Vordzenbachenhorn (E)	646625	142850	2820	1269	Aletschgletscher
17	Vordzen Rothorn (S)	646175	141875	2810	1269	Aletschgletscher
18	Geisshorn (SE)	645175	141250	2800	1269	Aletschgletscher
19	Grossfusshorn (SE)	643700	140550	2790	1269	Aletschgletscher
20	Grossfusshorn (SW)	643150	140675	2800	1269	Aletschgletscher
21	Sparrhorn	642025	138800	2780	1269	Aletschgletscher
22	Olmenhorn (SE)	647575	144275	2820	1269	Aletschgletscher
23	Eggishorn (NE)	650775	142575	2680	1269	Aletschgletscher
24	Strahlhorn (S)	650275	144450	2820	1269	Aletschgletscher
25	Bettmerhorn (S)	649100	140200	2690	1269	Aletschgletscher
26	Distelberg	640900	143425	2840	1269	Aletschgletscher
27	Oberaletschhutte	641450	141800	2820	1269	Aletschgletscher
28	Hohstock	640700	138475	2750	1269	Aletschgletscher
29	Grisighorn	639075	137250	2820	1269	Aletschgletscher
30	Risihorn	655025	145225	2660	1270	Binntal
31	Schwarzegge	665700	143150	2690	1270	Binntal
32	Albrun	666575	136325	2650	1290	Binntal
33	Tochuhorn	643925	123325	2500	1289	Brig
34	Schwarzhorn (E)	629075	132775	2500	1288	Raron
35	Hufjegrat	629250	133725	2560	1288	Raron
36	Wiwannihorn (SW)	631375	133225	2550	1288	Raron
37	Ougstchummuhorn (W)	631300	132425	2500	1288	Raron
38	Maelchgrat	635950	132275	2540	1288	Raron
39	Garsthorn	637200	132225	2560	1288	Raron
40	Schiltfurgga	637075	133475	2600	1288	Raron
41	Wiwannihorn (W)	632725	133800	2560	1288	Raron
42	Laegundegrat (Saas)	634150	114500	2580	1308	St. Niklaus
43	Mittleberg	629900	111725	2660	1308	St. Niklaus
44	Wasuhorn	625625	112825	2640	1308	St. Niklaus
45	Glatthorn	648100	117950	2200	1309	Simplon
46	Wysbodenhorn (NW)	644450	118400	2300	1309	Simplon
47	Wysbodenhorn (SE)	645350	117850	2220	1309	Simplon
48	Bodmerhorn	646350	115700	2160	1309	Simplon
49	Guggilhorn	650225	113900	2060	1309	Simplon
50	Trifthorn (W)	640950	106425	2640	1329	Saas

TL-ID	LOCATION	X-COORD	Y-COORD	Elevation (Z)	MAP_#	MAP_NAME
51	Trifthorn (S)	641975	106525	2760	1329	Saas
52	Trifthorn (SE)	642525	106500	2800	1329	Saas
53	Dri Hornli	643575	106425	2880	1329	Saas
54	Untershorn	641625	104925	2680	1329	Saas
55	Mittaghorn	639050	104125	2700	1329	Saas
56	Egginer	638775	102700	2820	1329	Saas
57	Kl Allain	638950	101100	2860	1329	Saas
58	Schwarzbergkopf	638950	99175	2880	1329	Saas
59	Punta Turiggia	648100	103200	2250	1329	Saas
60	Cimidi Pozzuoli	649300	104025	2100	1329	Saas
61	Zibelenfluehorn	648600	107675	2500	1329	Saas
62	Schijenhorn	649200	108225	2420	1329	Saas
63	Balmahorn	650175	109200	2340	1329	Saas
64	Guglen	635250	105500	2900	1328	Randa
65	Brunegghorn	625300	108475	2760	1328	Randa
66	Weisshornhutte	623600	103850	2920	1328	Randa
67	Pte Dent de Veisivi (NW)	605825	101525	2480	1327	Evolene
68	Pte Dent de Veisivi (NE)	606225	101375	2480	1327	Evolene
69	Pte Dent de Veisivi (E-N)	607200	100950	2500	1327	Evolene
70	Pte Dent de Veisivi (E-NE)	607575	100475	2540	1327	Evolene
71	Pte Dent de Veisivi (E-E)	607725	100000	2660	1327	Evolene
72	Pte Dent de Veisivi (E-S)	608100	99200	2700	1327	Evolene
73	Pte des Genevois	607775	98300	2800	1327	Evolene
74	M. Mine	609325	98225	2780	1327	Evolene
75	La Maya	610100	100225	2740	1327	Evolene
76	Ptes de Mourt	609425	101600	2640	1327	Evolene
77	La Rousette	602300	98875	2560	1326	Rosablanche
78	Le Veudale (SW)	558075	100775	2470	1324	Barbarine
79	Le Veudale (NE)	558175	100825	2440	1324	Barbarine
80	Pte de L'Ifala	558975	100525	2460	1324	Barbarine
81	Aig du Van (NW)	559475	101000	2400	1324	Barbarine
82	Aig du Van (NE)	560025	101250	2300	1324	Barbarine
83	Aig du Van (SE)	560125	100700	2240	1324	Barbarine
84	Le Charmo	559400	99475	2300	1324	Barbarine
85	Bel Oiseau	561225	102625	2260	1324	Barbarine
86	Tete des Ottans	560675	104300	2500	1324	Barbarine
87	Dt de Fenestral	562850	104525	2200	1324	Barbarine
88	Aig de Berard	554125	93300	2400	1344	Col de Balme
89	Tete du Bechat	553925	91500	2380	1344	Col de Balme
90	Aig de Charlano	554075	89450	2340	1344	Col de Balme
91	Pointe des Vioz	553650	88450	2220	1344	Col de Balme
92	Aig de la Remua	B558600	93825	2300	1344	Col de Balme
93	Aig de Tete Plate	557100	93025	2520	1344	Col de Balme
94	Aig de Belvedere	B557275	91625	2300	1344	Col de Balme
95	Tete des Evettes	B556275	90325	2200	1344	Col de Balme
96	Arete Sup de Charlano B	555025	88825	2200	1344	Col de Balme
97	Plan Praz (le Brevant) B	554125	87525	2200	1344	Col de Balme
98	Mer de Glace (W) B	559025	86125	2300	1344	Col de Balme
99	Aig a Brochard (Mer de Glace E) B	560275	88875	2200	1344	Col de Balme
100	Aig a Brochard up (Mer de Glace E) B	560600	88050	2200	1344	Col de Balme
101	Arete des Flames de Pierre B	561025	86075	2400	1344	Col de Balme
102	Aig des Gds Monetets B	562850	90275	2500	1344	Col de Balme

TL-ID	LOCATION	X-COORD	Y-COORD	Elevation (Z)	MAP_#	MAP_NAME
103	Bec de Lachat B	562625	92925	2400	1344	Col de Balme
104	Bec Rouge Superieur B	563700	91825	2500	1344	Col de Balme
105	Bec du Picheu	563725	95000	2400	1344	Col de Balme
106	Les grandes Otanes (NW)	563900	97150	2300	1344	Col de Balme
107	Les grandes Otanes (N)	564650	97350	2280	1344	Col de Balme
108	Cornes de Loria	557725	97750	2500	1344	Col de Balme
109	Le Chatelet	573975	94025	2300	1345	Orsieres
110	Pointes des Chevrettes	572475	94175	2400	1345	Orsieres
111	Clochiers du Portalet	571150	92850	2600	1345	Orsieres
112	Petite Pte des Planereuses	573125	91250	2380	1345	Orsieres
113	Pointes des Six Niers	572450	87925	2420	1345	Orsieres
114	La Maye	572075	86200	2440	1345	Orsieres
115	Mulets de la Lia	592125	93225	2680	1346	Chanrion
116	La Grande Ashle	593800	94525	2700	1346	Chanrion
117	Pointe d'Otemma (S)	596800	86925	2880	1346	Chanrion
118	Pointe d'Otemma (W)	596100	88050	2820	1346	Chanrion
119	Tour de Boussine (E)	592850	87550	2860	1346	Chanrion
120	Aretes de Lire Rose	595675	90500	2780	1346	Chanrion
121	Vuibe (N)	603175	94675	2600	1347	Matterhorn
122	Vuibe (MID)	603275	94450	2630	1347	Matterhorn
123	Vuibe (S)	603325	94200	2640	1347	Matterhorn
124	La Maya (N)	604350	95975	2590	1347	Matterhorn
125	La Maya (S)	604550	95600	2640	1347	Matterhorn
126	Doves Blanches	604875	94475	2720	1347	Matterhorn
127	Tete des Roeses	610200	88750	2900	1347	Matterhorn
128	Pte Budden	610075	87200	2860	1347	Matterhorn
129	Gran Vanna	607250	86775	2800	1347	Matterhorn
130	Crete du Plan	605625	93800	2820	1347	Matterhorn
131	Untergabelhorn	620500	96625	3000	1348	Zermatt
132	Pizzo Nero	640925	88450	2300	1349	Monte Moro
133	Faderhorn	639675	92450	2400	1349	Monte Moro
134	P. S. Pietro	642200	93875	2900	1349	Monte Moro
135	Pte Fiorio	593625	78475	2580	1366	Mont Velan
136	Mt du Clapy	594400	79425	2600	1366	Mont Velan
137	M de Crete Seche	597250	81750	2660	1366	Mont Velan
138	M de Chamontane	598575	82075	2700	1366	Mont Velan
139	Becca de Chatelet	601550	83500	2740	1366	Mont Velan
140	M Gele (SW)	593325	82625	2720	1366	Mont Velan
141	Pointe d'Ayace	595375	85200	2900	1366	Mont Velan
142	Pte Allobrogia	570925	83350	2750	1365	Gd St-Bernard
143	Aig Rouge de Triolet* PO	569875	82600	2800	1365	Gd St-Bernard
144	M de Greuvettaz* PO	569150	82575	2750	1365	Gd St-Bernard
145	Grand Chenalette (E)	579550	80550	2500	1365	Gd St-Bernard
146	Becs Noir	581275	82075	2460	1365	Gd St-Bernard
147	Comba	577575	78925	2400	1365	Gd St-Bernard
148	M Mort (W)	578900	79225	2650	1365	Gd St-Bernard
149	Pte Gerlach	604250	84850	2770	293	Valpelline
150	Aig Rouge (Becca des Lacs)	605550	85700	2790	293	Valpelline
151	M Dragon	608950	85250	2800	293	Valpelline
152	Pte des Fontanelles	608100	84700	2800	293	Valpelline
153	M Charvin	607200	83750	2780	293	Valpelline
154	M Dzalou	603200	81400	2700	293	Valpelline

TL-ID	LOCATION	X-COORD	Y-COORD	Elevation (Z)	MAP_#	MAP_NAME
155	Aig de L'Eveque* PO	566275	78625	2725	292	Courmayeur
156	Pte Walker* PO	565350	78050	2750	292	Courmayeur
157	M de Rochefort* PO	563600	77400	2800	292	Courmayeur
158	Tour de Jethoula* PO	562100	76700	2750	292	Courmayeur
159	M Rouge de Peuterey* (NE) PO	558350	72575	2700	292	Courmayeur
160	M Rouge de Peuterey* (SW) PO	557625	72075	2750	292	Courmayeur
161	Aig de Breuillat* PO	555850	71525	2750	292	Courmayeur
162	Aig de Combal* PO	553250	70175	2775	292	Courmayeur
163	Tete Entre Deux Sex	568950	76200	2500	292	Courmayeur
164	Tete de Bernarde	566950	75075	2500	292	Courmayeur
165	Glace (Aig de l'M) B	559540	84950	2400	292	Courmayeur
166	Glace (Aig de la Trelaporte) B	560600	84150	2550	292	Courmayeur
167	Glace (Aig du Grepon) B	559950	82900	2650	292	Courmayeur
168	Glace (Aig du Tacul) B	562400	82150	2750	292	Courmayeur
169	Nid d'Aigle	550800	79700	2250	46	Val de Bagnes
170	Dreieckhorn (NE ridge)	645900	148750	2900	1249	Finsteraarhorn
171	Konkordiahutten	647250	150075	2900	1249	Finsteraarhorn
172	Chamm (SW ridge)	648225	148925	2900	1249	Finsteraarhorn
173	Herbrigat	649225	147600	2890	1249	Finsteraarhorn
174	Gruenegg (SW ridge)	646925	150875	3000	1249	Finsteraarhorn
175	Gruenegg (S ridge)	647600	151350	3100	1249	Finsteraarhorn

